Department of Applied Mechanics

Modeling ductile fracture in ship structures with shell elements

Mihkel Kõrgesaar

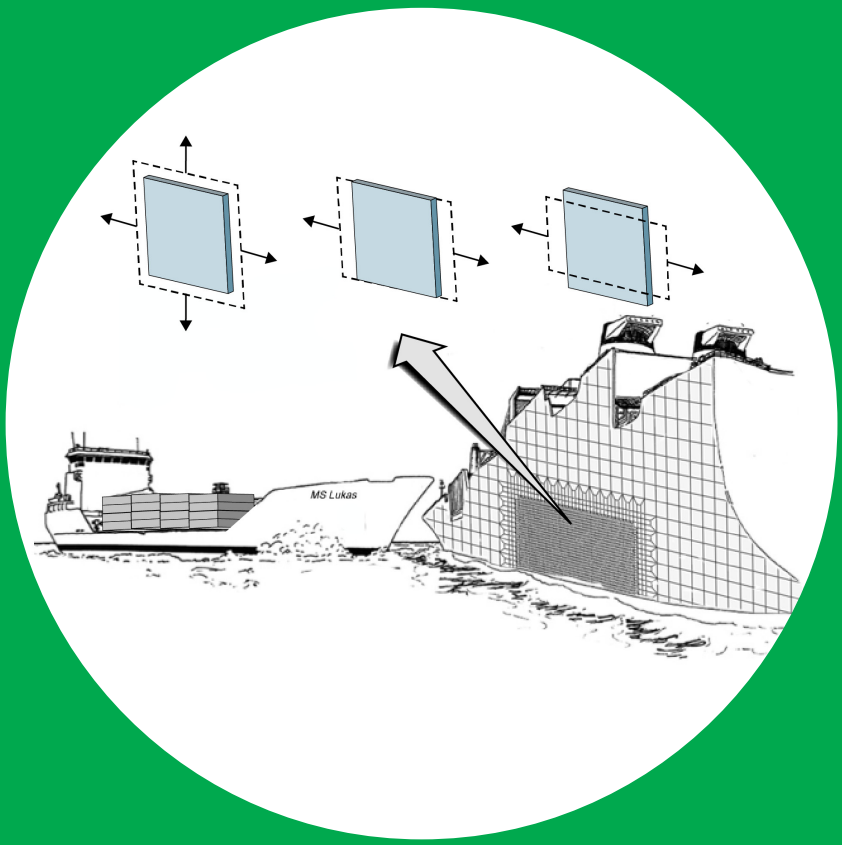

Aalto University

DOCTORAL DISSERTATIONS

Aalto University publication series
DOCTORAL DISSERTATIONS 22/2015

Modeling ductile fracture in ship structures with shell elements

Mihkel Kõrgesaar

A doctoral dissertation completed for the degree of Doctor of Science (Technology) to be defended, with the permission of the Aalto University School of Engineering, at a public examination held at the lecture hall 216 of the school on 17 April 2015 at 12.

Aalto University
School of Engineering
Department of Applied Mechanics
Marine Technology

Supervising professor
Prof. Jani Romanoff

Thesis advisor
Prof. Heikki Remes

Preliminary examiners
Prof. Manolis S. Samuelides, National Technical University of Athens, Greece

Dr. George Wang, American Bureau of Shipping, USA

Opponent
Prof. Jørgen Amdahl, Norwegian university of science and technology, Norway

Aalto University publication series
DOCTORAL DISSERTATIONS 22/2015

ISBN 978-952-60-6084-2 (printed)
ISBN 978-952-60-6085-9 (pdf)
ISSN-L 1799-4934
ISSN 1799-4934 (printed)
ISSN 1799-4942 (pdf)
http://urn.fi/URN:ISBN:978-952-60-6085-9

Images: 19

Unigrafia Oy
Helsinki 2015

Finland

Publication orders (printed book):
mihkel.korgesaar@aalto.fi

Aalto University

Abstract

Aalto University, P.O. Box 11000, FI-00076 Aalto www.aalto.fi

Author
Mihkel Kõrgesaar

Name of the doctoral dissertation
Modeling ductile fracture in ship structures with shell elements

Publisher School of Engineering

Unit Department of Applied Mechanics

Series Aalto University publication series DOCTORAL DISSERTATIONS 22/2015

Field of research Marine structures

Manuscript submitted 2 October 2014 **Date of the defence** 17 April 2015

Permission to publish granted (date) 26 January 2015 **Language** English

☐ **Monograph** ☒ **Article dissertation (summary + original articles)**

Abstract

Large thin-walled structures provide the means for cost and energy efficiency in structural design. The design of such structures for crash resistance requires reliable FE simulations. In these simulations large plane stress shell elements are used. Simulations require the knowledge of the true stress–strain response of the material until fracture initiation and beyond. Because of the size effect, local material relation determined with experiments is not applicable to large shell elements. The mesh size dependency arises because of the high stress and strain gradients preceding the ductile fracture of metals. Essentially, plane stress shell elements require the equivalent average plane stress material curve. The fact that the stress state in the material affects the fracture ductility further complicates the analysis.

This thesis investigates the damage process of shell elements under multi-axial tension. Emphasis is placed on the combined effects of stress state and element size. A novel numerical approach is presented that provides an equivalent plane stress material curve up to the point of fracture initiation for large shell elements under multi-axial tension loading. The fracture initiation strain is found to scale in combination with stress state and element size. Mesh size dependence is shown to be weaker in plane strain and equi-biaxial tension than in uniaxial tension. Simulations employing this scaling yield very good convergence in panel analysis with different mesh densities.

The results also demonstrate that the equivalent plane stress material curve is of a softening type. Softening characterizes consecutive stages of the damage process in large elements: necking, fracture initiation, and propagation. A method is presented to calibrate the damage parameters describing softening for the tearing type of crack propagation under in-plane loading. The damage parameters depend on element size and on the failure mode; that is, how the fracture initiates and under which conditions the crack starts to propagate. The softening model calibrated for stiffened panels is used to simulate a ship collision accident. The simulations showed that softening effectively reduces the mesh dependency. However, it is very complicated to define proper calibration parameters a priori for real structures. Therefore, in crashworthiness analysis where importance is on absorbed energy of the structure, fracture models based on sudden element deletion remain attractive for practical engineering work.

The presented fracture modeling approach is applicable to slender shell structures in which fracture initiation and tearing in membrane state dominate the structural response. Approach should be extended for bending dominated problems and other materials such as welds in the future.

Keywords finite elements, fracture, softening, size effects

ISBN (printed) 978-952-60-6084-2 **ISBN (pdf)** 978-952-60-6085-9

ISSN-L 1799-4934 **ISSN (printed)** 1799-4934 **ISSN (pdf)** 1799-4942

Location of publisher Helsinki **Location of printing** Helsinki **Year** 2015

Pages 121 **urn** http://urn.fi/URN:ISBN:978-952-60-6085-9

Preface

This thesis is based on work carried out at the Advanced Marine Structures research group in the Department of Applied Mechanics of Aalto University between 2010 and 2014. During the process I was financed by Aalto University School of Engineering and the National Graduate School in Engineering Mechanics, the Finnish National project FIMECC I&N, the Finnish Maritime Foundation, the EU-funded research project MIMIC and the Finland Distinguished Professor (FiDiPro) project "Non-linear Response of Large, Complex Thin-Walled Structures" funded by the Finnish Funding Agency for Innovation (Tekes), Deltamarin, Napa Ltd, Koneteknologiakeskus Turku, Ruukki and STX Finland. This financial support is gratefully acknowledged.

First, I would like to thank my supervisor Jani Romanoff for his extensive support, encouragement, and valuable discussions during the thesis process. His view on life and guidance in non-work-related matters has been a source of much energy. I will never forget this. I would like to thank my thesis advisor Heikki Remes for his consistent guidance, insightful comments, and constructive criticism. I am grateful to Petri Varsta and Sören Ehlers for evoking my interest in research, their guidance in the early stages of the research, and for encouraging me to continue with my studies. I also wish to thank my co-instructor Kristjan Tabri and Hendrik Naar from Tallinn University of Technology for constructive comments during the thesis process.

I would like to thank my colleagues: Ingrit Lillemäe, Jasmin Jelovica, Markus Ahola, Anghel Cernescu, Darko Frank, Pauli Lehto, Anssi Karttunen, Eero Avi and other post-graduate students from Applied Mechanics for their extensive support, helpfulness and for creating a pleasant working atmosphere. My gratitude also goes to Leila Silonsaari and Seija Latvala whose help with daily problems is recognized.

Finally, I would like to thank my family and friends, especially my wife Marii for staying with me in Finland, for her encouragement during the entire project and devotion to our family. Last but not least, I thank my son Lukas for the joy he has brought into everyday life.

Espoo, January 29, 2015,

Mihkel Kõrgesaar

Contents

List of Publications

This thesis consists of an overview and of the following publications which are referred to in the text by their Roman numerals.

I Kõrgesaar, Mihkel; Remes, Heikki; Romanoff, Jani. Size dependent response of large shell elements under in-plane tensile loading. *International Journal of Solids and Structures*, Volume 51, Issues 21-22, Pages 3752-3761, October 2014.

II Kõrgesaar, Mihkel; Romanoff, Jani. Influence of softening on fracture propagation in large-scale shell structures. *International Journal of Solids and Structures*, Volume 50, Issue 24, Pages 3911-3921, November 2013.

III Kõrgesaar, Mihkel; Romanoff, Jani. Influence of mesh size, stress triaxiality and damage induced softening on ductile fracture of large-scale shell structures. *Marine Structures*, Volume 38, Pages 1-17, October 2014.

IV Kõrgesaar, Mihkel; Tabri, Kristjan; Naar, Hendrik; Reinhold, Edvin. Ship collision simulations using different fracture criteria and mesh size. In *International Conference on Ocean, Offshore and Arctic Engineering OMAE2014*, San Francisco, USA, Paper no: OMAE2014-23576, June 8-13 2014.

V Kõrgesaar, Mihkel; Jelovica, Jasmin; Romanoff, Jani; Kurmiste, Andres. Steel sandwich panels optimized for crashworthiness: the X- and Y-core. In *International Conference on Thin-Walled Structures ICTWS 2014*, Busan, South Korea, Paper no: ICTWS2014-0509, 28 September - 2 October 2014.

Author's Contribution

Publication I: "Size dependent response of large shell elements under in-plane tensile loading"

The author developed a method to determine the element size dependent true stress and strain relation and fracture initiation strain for multi-axial tension condition. The author also prepared and analyzed the finite element models, investigated the influence of the mesh size and stress state on the fracture initiation strain, analyzed the results, and prepared the manuscript. Remes and Romanoff contributed to the manuscript with valuable comments and suggestions.

Publication II: "Influence of softening on fracture propagation in large-scale shell structures"

The author proposed the approach, prepared and analyzed the finite element models and the VUMAT subroutine including softening, analyzed the results and prepared the manuscript. Romanoff contributed to the manuscript with valuable comments and suggestions.

Publication III: "Influence of mesh size, stress triaxiality and damage induced softening on ductile fracture of large-scale shell structures"

The author prepared the finite element models, implemented the fracture criterion including softening into ABAQUS, analyzed the results, and prepared the manuscript. Romanoff contributed to the manuscript with valuable comments and suggestions.

Publication IV: "Ship collision simulations using different fracture criteria and mesh size"

The author carried out the finite element simulations, implemented different fracture criteria into ABAQUS, analyzed the results, and prepared the manuscript. Reinhold built the finite element models. Tabri and Naar con-

tributed to the manuscript with valuable comments and suggestions.

Publication V: "Steel sandwich panels optimized for crashworthiness: the X- and Y-core"

The author proposed the idea, carried out the finite element simulations, analyzed the optimization results and was the main contributor to the manuscript. Kurmiste built the parametric finite element models. Jelovica helped to set up the optimization problem and wrote the optimization chapter of the manuscript. Jelovica and Romanoff contributed to the manuscript with valuable comments and suggestions.

Original features

Ductile fracture in large structures such as ships is commonly analyzed with non-linear Finite Element (FE) simulations employing plane stress shell elements. In these simulations, the knowledge of the material behavior until fracture initiation and beyond is essential. However, the complexity of such analysis arises from the range of scales involved. Applying the material response until fracture initiation determined with small test specimens to large shell elements, which are used in the analysis of large structures, is not straightforward because of the mesh size effect. The mesh size effect arises as a result of the averaging of local stress and strain gradients, which are characteristic of ductile fracture, over large shell elements. The following features of this thesis are believed to be original:

1. A generic, numerical approach is developed in [PI] which allows determination of the equivalent plane stress material curve until fracture initiation. Results show that the mesh size effect is stronger in uniaxial tension than in plane strain and equi-biaxial tension.

2. PI shows that stress state has small influence on fracture initiation strain in large shell elements between uniaxial and plane strain tension. This is important since PIV shows that in large-scale collision simulations the majority of elements fail between uniaxial and plane strain tension.

3. An energy density-based averaging unit concept is developed to determine the damage parameters for the softening type of true stress-strain curve for propagating cracks in large shell elements under Mode I tearing [PII]. The damage parameters describing softening are shown to depend on the mesh size [PII] and the mode in which the fracture initiates and propagates [PII, PIII]. Large-scale ship collision simulations with different element sizes indicate that softening helps to get better convergence with larger shell elements, i.e. remove mesh size effect [PIV].

4. Indentation simulations with large-scale panels [PIII] demonstrated that the scaling of the fracture initiation strain on the basis of both the stress state and element size [PI] can more accurately predict the energy for fracture in comparison with the state-of-the-art methods.

5. It is shown that in novel crashworthy structures, such as sandwich panels, impact energy is mostly absorbed by bending due to buckling and folding

mechanisms [PV], instead of fracture and tearing observed in traditional stiffened panels. Moreover, the bending gradients are the highest close to the welds where material properties change rapidly. This perspective brings out the limitations of the present fracture modeling approach, and thus, sets directions for future work.

List of symbols and abbreviations

A	Actual cross-section area of the tensile specimen
A_0	Initial cross-section area of the tensile specimen
D	Damage indicator
D_0	Damage initiation parameter
D_c	Critical damage parameter
J_2	Second invariant of deviatoric stress tensor
L	Tensile specimen length
L_e	Element length
t	Plate thickness
L_e/t	Dimensionless element size
m	Parameter controlling non-linearity of the softening process
ε	Engineering strain
$\overline{\varepsilon}$	Equivalent plastic strain
$\overline{\varepsilon}_f$	Equivalent plastic strain to fracture initiation
η	Stress triaxiality
η_a	Average stress triaxiality
σ	Engineering stress
σ_h	Hydrostatic stress
$\overline{\sigma}$	Equivalent stress
$\sigma_{1,2,3}$	First, second and third principal stress
ALS	Accidental limit state
AU	Averaging unit
BWH	Bressan-Williams-Hill instability criterion
EBT	Equi-biaxial tension
FE	Finite Element
FEM	Finite Element Method
FLD	Forming limit diagram
GL	Germanischer Lloyd
IMO	International Maritime Organization
PST	Plane strain tension
PI, PII, ..., PV	Publication I, Publication II, ..., Publication V
RTCL	Rice-Tracey-Cockcroft-Latham fracture criterion
RVE	Representative volume element
SOLAS	Safety Of Life At Sea
UAT	Uniaxial tension

1. Introduction

1.1 Background

The structural safety of large-scale shell structures has become more important as a result of the increased societal awareness regarding accidents and structural failure. It can be increased by exploiting novel design methods and advanced structures. The design of ship structures must satisfy commercial requirements, while at the same time complying with the international rules set by the Classification Societies, as well as satisfying the safety regulations set by the International Maritime Organization (IMO). The classification rules, together with SOLAS (*Safety Of Life at Sea*, IMO convention, 2006), define the minimum structural requirements a vessel must satisfy to be safely constructed and operated.

The full potential of structures can be realized through advanced strength assessment methods. Moreover, these novel methods are the basis for the evolution of better design standards and international regulations. One particular example is the accurate assessment of structural strength under extreme conditions, such as during a ship collision or grounding, i.e. accidental limit state (ALS). Detecting and explaining the most important factors influencing the accuracy is the basis for novel assessment methodologies and for future developments.

During a ship collision or grounding, the steel structure can rupture in a ductile manner. The ductility of the material characterizes its ability to undergo large plastic deformations without fracture. Today, the structural response under extreme loads involving ductile fracture is determined with non-linear finite element (FE) simulations. FE simulations require the input of the true stress-strain relation until the point of fracture initiation. This material behavior is determined with the tensile test; see Figure 1.1. In the context of a displacement controlled tensile test, fracture initiation is defined as the point where the crack is clearly visible, followed by a sudden load drop resulting in splitting of the specimen into two. In this thesis, the equivalent von Mises plastic strain at fracture initiation $\bar{\varepsilon}_f$ is denoted as the “fracture initiation strain”; see Figure 1.1 (B). The “fracture criterion”, on the other hand, specifies the fracture initiation strain as a function of some measurable parameters.

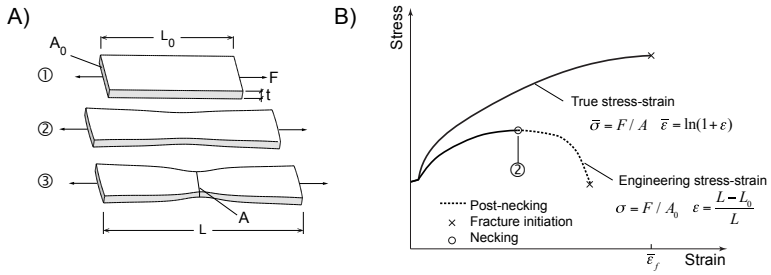

Figure 1.1. A) Stages of tensile test. B) True and engineering stress-strain curve.

A common practice in FE simulations is to remove a finite element once its fracture strain is reached (ISSC, 2006). Therefore, in the context of a FE analysis, where fracture is simulated by element removal, "fracture initiation" implies the removal of a first element in the simulation, while the term "fracture propagation" refers to the subsequent removal of other elements[1]. Throughout this thesis, this fracture modeling approach is referred to as *sudden element removal*; fracture criteria that employ this approach are referred to as *sudden models*. Alternatively, the fracture process can be described as a continuous degradation of element strength using softening type of constitutive law, where stress decreases to zero for increasing strain specifying the element removal. Terminology used with softening model is different than used in sudden models; detailed explanation is given at the end of this chapter and in Figure 1.5.

The material relation and fracture initiation strain determined with a tensile test depend on the gauge length; see Figure 1.2. In order to employ this material relation and fracture strain in simulations, the dimensionless element size[2], i.e., the element length to thickness ratio L_e/t, must remain equivalent to the gauge length divided by the plate thickness ratio. In other words, fracture strain is mesh size dependent. In addition, fracture strain depends on the stress state in the material; this notion will be further elaborated in the next section. Current software and hardware capabilities prohibit the detailed modeling of the fracture process in large structures. Large plane stress shell elements with an element size around $L_e/t \geq 5$ are typically used in these simulations, as shown in Figure 1.2. In ship structures the minimum rule plate thickness can be as thin as 5 mm, which, according to the above ratio, gives a minimum element length of $L_e = 25$ mm. Such large shell elements have to resolve in the average sense, at the macro-scale, the ductile material damage process, which takes place in three dimensions. The ductile material damage process at the macro-scale can be divided into three separate stages:

[1] Element is removed when fracture criterion is satisfied in all section points at any integration point. This is the default option in ABAQUS Explicit.

[2] For the sake of brevity, dimensionless element size will be referred to as element size or equivalently, mesh size in the rest of the thesis.

necking, fracture initiation, and fracture propagation. Because of dependence of fracture initiation strain on mesh size the material relation and fracture initiation strain determined experimentally with test specimens are not directly applicable to simulation of large structures. The question arises as to how to determine the structural response using large shell elements, without losing details of the material damage process observed in test specimens.

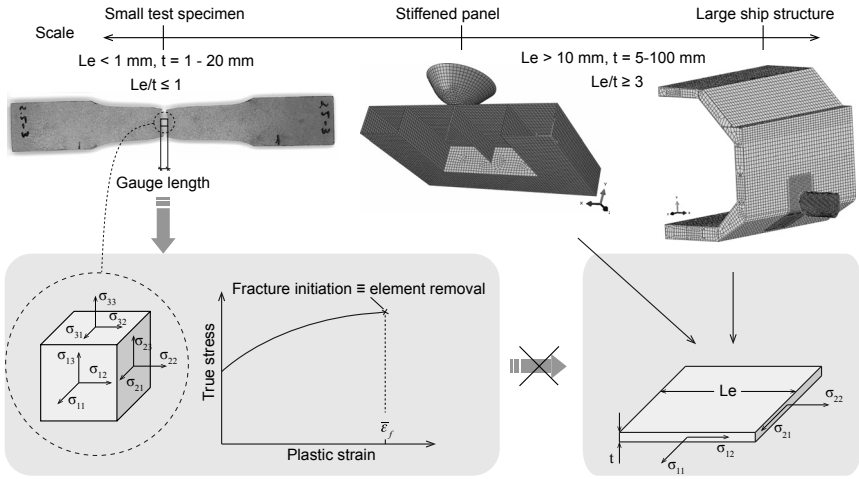

Figure 1.2. Illustration of the different scales in fracture analysis: small test specimen, stiffened panel and large-scale ship structure.

Different approaches exist to overcome the scale issue, but the damage mechanics behind those approaches has often been overlooked. Consequently, there is considerable uncertainty in different fracture criteria, especially on how they account for the mesh size dependence and stress state. In this thesis, a systematic approach is proposed to determine the fracture initiation strain and the equivalent plane stress material curve for different element sizes and stress states. This equivalent material curve is further extended to represent the whole damage process of the material, including necking, fracture initiation and propagation, in a single large shell element. The impact on prediction of structural behavior of large structures is presented, and suggestions for future work are given.

1.2 State of the art

Ductile fracture of metals is a complicated process and requires detailed investigations of the microstructure of the material (Woelke and Abboud, 2012). Fracture process in the microstructural level involves nucleation, growth and coalescence of voids (Garrison and Moody, 1987; Tasan et al., 2009; Benzerga and Leblond, 2010). Growth and coalescence can be investigated using unit cell models where the scale of the analyzed problem is consistent with the grain

size (Gurson, 1977; Barsoum and Faleskog, 2007; Dunand and Mohr, 2014; Tvergaard, 2014). In the analysis of large engineering structures the range of scale is several orders of magnitudes higher, which makes the use of these models prohibitive because of the computational reasons.

One approach to upscale the non-linear behaviour of a well-characterized microstructure is to employ multi-scale methods, and in particular computational homogenization (Coenen et al., 2012). However, this technique is computationally expensive, requires a well-defined microstructure as well as premature knowledge of the crack path (Geers et al., 2010). In recent years, the concept of a cohesive zone ahead of the crack tip generalized as cohesive zone models, introduced by Dugdale (1960) and Barenblatt (1962), have been used for crack propagation problems. In this modeling approach special interface elements obeying a cohesive law are introduced between the standard finite elements allowing for inter-element separation. The practical applications of cohesive zone models however, are still limited to problems where the crack path is known a priori; for example, welded structures (Schreider and Brocks, 2006) and post-mortem analysis of panels (Nielsen and Hutchinson, 2012; Woelke et al., 2013). The fact that crack path must be known a priori make these methods unsuitable for design analysis of large structures such as ship, as ships contain numerous discontinuous structural elements, can experience variety of loads simultaneously and have welds – all affecting the crack path.

In general, a ductile fracture in a metal sheet is preceded by a loss of stability (Marciniak and Kuczynski, 1967; Hutchinson and Neale, 1979; Hu et al., 2002; Xue, 2010). This phenomenon is also known as necking. At and around the local area of neck, the stress state becomes three-dimensional, as the material is in plastic stage and high stress and strain gradients appear, as shown in Figure 1.3 (A). Outside of the necked region unloading of the sheet can take place. Experimental evidence for such gradients is presented in several studies, e.g., Wattrisse et al. (2001), Hogström et al. (2009), Ehlers and Varsta (2009), Tardif and Kyriakides (2012). Because of the necking and accompanied strain gradients the true stress-strain curves in Figure 1.3 (B) are element size dependent. As demonstrated in Figure 1.3 (C), the fracture initiation strain decreases with increasing element size as the average is taken over a larger area.

There are two popular approaches to account for the mesh size. Both are based on the standard tensile experiment with dog-bone specimens. In the first approach, the size of the finite element is set to be equal with the certain gauge length over which strains are averaged (Hogström et al., 2009; Ehlers and Varsta, 2009); Figure 1.3 (A). Thereby, the measured fracture initiation strain can be directly employed in the FE simulation. The true stress, on the other hand, cannot be directly measured, which is why it is calculated using the

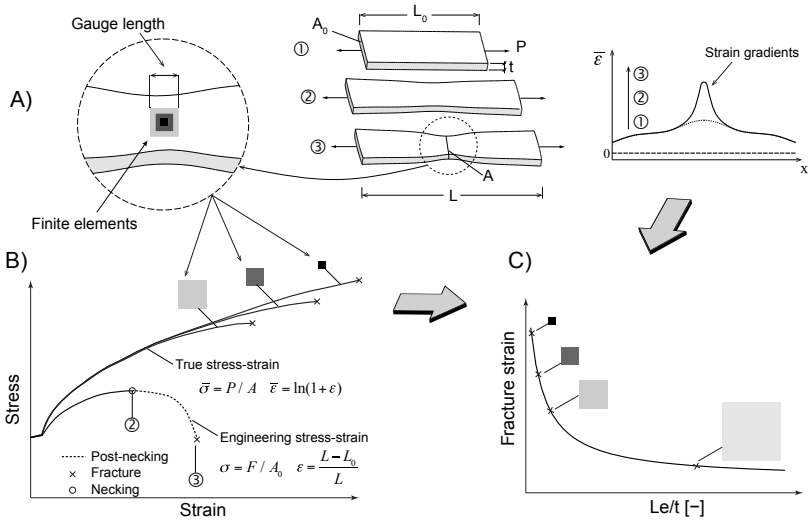

Figure 1.3. Origin of size effects. A) Standard tensile test. B) Engineering and true stress-strain curves. C) Dependence of fracture strain on finite element size – Barba's law.

minimum cross-sectional area of the specimen[3]. The alternative, an iterative approach, focusses on accurate prediction of fracture initiation strain only. For one selected element size, agreement between the numerical simulation and the tensile experiment is achieved by iteratively changing the fracture initiation strain until compliance between simulation and experiment is achieved; see, e.g., Zhang et al. (1999), and Simonsen and Lauridsen (2000). As a result, the true stress-strain relation until the point of fracture initiation is obtained for larger elements, as shown in Figure 1.3 (B). Both approaches can be used for different element sizes, yielding a relation displayed in Figure 1.3 (C), which prescribes how to scale the fracture strain according to the element size L_e/t. This scaling law derived on the basis of a uniaxial tension test is known as Barba's law. The fracture criterion that is based on the critical equivalent plastic strain and is scaled with Barba's law is referred as the *shear*[4] criterion. The simplicity of the *shear* criterion stems from the assumption that the stress state in the material has no effect on the scaled fracture initiation strain. Because of its simplicity, this is one of the most frequently employed fracture criterion in ship collision and grounding analysis, see the review article by Samuelides (2012) and the recent proceedings of the International Conference on Collision and Grounding of Ships and Offshore Structures (Amdahl et al., 2013).

The commonly applied *shear* criterion and the scaling procedure in the form of Barba's law are valid only under uniaxial tension. However, in structures

[3]Hogström et al. (2009) measured this minimum cross-sectional area at the fracture location while Ehlers and Varsta (2009) measured it as a function of the gauge length.

[4]The name *shear* stems from the fact that the von Mises equivalent plastic strain is used, whereas the von Mises yield criterion is based on the critical shear strain energy at the tensile yield point (Rees, 2006)

the stress state can deviate from uniaxial tension as a result of the changing load conditions and structural topologies, e.g., a stiffened plate. Under multi-axial stressing, fracture ductility depends markedly on the hydrostatic stress ($\sigma_h = (\sigma_1 + \sigma_2 + \sigma_3)/3$; where σ_1, σ_2 and σ_3 are the principal stresses) or the stress triaxiality η (hydrostatic stress divided by the equivalent von Mises stress $\bar{\sigma} = \sqrt{3J_2}$, where J_2 is the second invariant of the deviatoric stress tensor) as first observed by McClintock (1968), Rice and Tracey (1969), and Johnson and Cook (1985) and more recently shown in various experimental studies, e.g., Bao and Wierzbicki (2004), Wierzbicki et al. (2005), Barsoum and Faleskog (2007), Choung et al. (2012), and Haltom et al. (2013). An example of the influence of triaxiality on the fracture initiation strain in plane stress condition is shown for steel in Figure 1.4 (A) (Bai and Wierzbicki, 2010). Figure 1.4 (B) shows the stress states considered in this thesis. Plane strain tension arises as a special case for these shell elements in direction 1 (σ_3 = 0 and ε_1 = 0), as opposed to through thickness direction commonly assumed (direction 3, ε_3 = 0), see Bai (2008). Similar relationships have been presented for other metals, e.g. aluminum (Lou et al., 2012). This curve applies to a local scale, i.e., $L_e/t <$ 1, and is obtained through extensive experimental numerical study. From the list of important features displayed in Figure 1.4 (A) one is highlighted: fracture ductility is lowest in plane strain tension, $\eta = \sqrt{1/3}$.

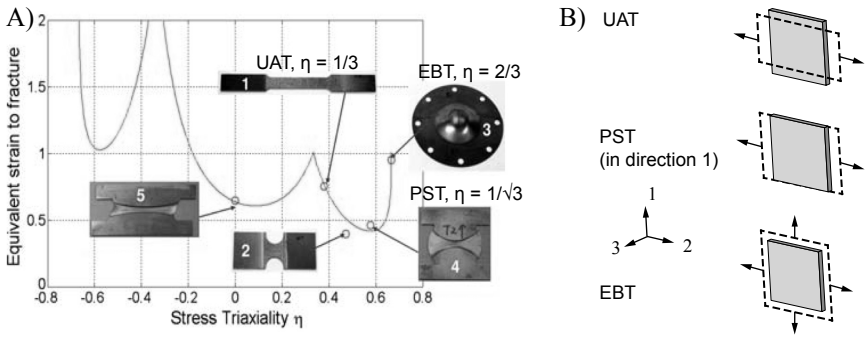

Figure 1.4. A) Influence of stress triaxiality on fracture initiation strain for TRIP steel (Bai and Wierzbicki, 2010): uniaxial tension (UAT), plane strain tension (PST), equi-biaxial tension (EBT). B) Stress state extremes considered in detail in this thesis.

It is generally agreed that the *shear* criterion is appropriate for crash simulations of large structures, e.g., ships (Hogström and Ringsberg, 2012; Ehlers, 2010), where the overall, or global, force-displacement response can be predicted satisfactorily. This gives false confidence and disguises its accuracy for predicting fracture with smaller elements, where Barba's law scaling and *shear* criterion have yielded inconsistent results (Alsos et al., 2009; Villavicencio et al., 2013).

The fracture criteria adopted by the Classification Societies are also stress state independent. Det Norske Veritas (DNV, 2013) recommends a constant

fracture initiation strain. Germanischer Lloyd (GL) uses a criterion that is very similar to the *shear* criterion (Zhang et al., 2004; Scharrer et al., 2002) and where the critical thinning strain values are deduced from the thickness measurements of a standard tensile test. To account for the mesh size effect the criterion is scaled proportionally with the element size, L_e/t.

Some of the fracture criteria employed in large-scale structural analysis recognize the importance of stress triaxiality on the fracture initiation strain. One set of such criteria belongs to forming limit diagrams (FLD) that define the critical strain or stress levels, which should not be exceeded in order to avoid the localized necking and fracture of thin sheets. Since mesh size effect appears after necking, these criteria are often assumed to be mesh size independent, e.g., the Bressan-Williams-Hill (BWH) instability criterion (Alsos et al., 2008). Although this simplifies the implementation into FE codes, the approach has been criticized because the post-necking energy under the stress-strain curve is neglected; see Figure 1.1. Hence, analyses with FLD (Hogström and Ringsberg, 2012) and with the BWH criterion (Alsos et al., 2009) have yielded conservative results. To introduce mesh size sensitivity into analysis with FLD, Woelke and Abboud (2012) scale post-necking energy to fracture initiation linearly with element size independently of the stress state; see also (Woelke et al., 2013). Another fracture criterion is the Rice-Tracey-Cockcroft-Latham (RTCL) damage criterion (Urban, 2003; Törnqvist, 2003). The fracture initiation strain given by the RTCL criterion is scaled for different element sizes on the basis of the fracture initiation strain determined with the uniaxial tension test, i.e., with Barba's law.

Although the above-mentioned criteria are stress state dependent and hence more advanced than the *shear* criterion, the mesh size effect is accounted for on the basis of the uniaxial tensile test. However, besides the clear influence of stress triaxiality on the fracture strain, it can similarly affect the scaling law, which is not considered by these criteria. In other words, the mesh size effect might be affected by the stress state, which in turn would make Barba's law scaling inapplicable to other stress states besides uniaxial tension. Walters (2014) has proposed scaling the fracture initiation strain on the basis of both the element size and stress triaxiality. He combines two well-known failure criteria for small and large elements. As a lower bound of the failure criteria he uses Swift's (1952) necking criterion; this is used for high L_e/t-ratios. The upper bound is Bai and Wierzbicki's (2010) failure criterion. In between these extremes he scales the fracture strain according to the element size L_e/t and stress triaxiality η. However, no physical justification for this approach is given.

When the element in the simulation satisfies the fracture criterion and is removed from the simulation, the load carried by this element is redistributed to the neighboring elements. Consequently, fracture propagation is a discontinu-

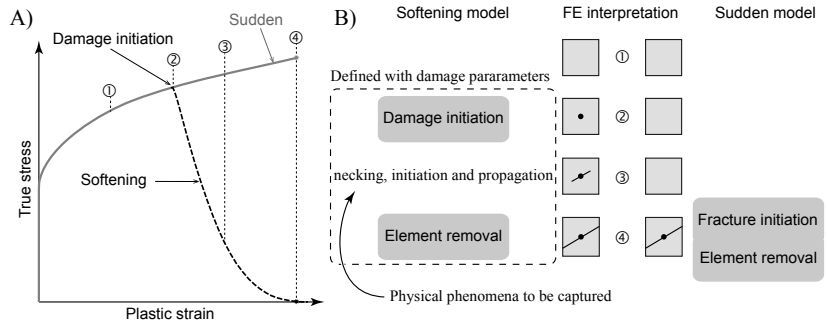

Figure 1.5. A) Sudden versus softening type of equivalent material model for shell elements. B) Terminology used in this thesis to distinguish between different models.

ous process when the standard hardening type of material relation is used – see Figure 1.2 – since load-carrying element is removed suddenly at the maximum stress. This is especially true when elements become large, $L_e/t > 10$. The problem is partly solved by coupling the material model with the fracture model. Essentially, a softening type of true stress and strain relation is introduced, as illustrated in Figure 1.5 (A), which allows the element stiffness to be reduced gradually (Lemaitre, 1985; Lemaitre, 1996). With continuous degradation of element stiffness, or softening, an attempt is made to phenomenologically model material damage process and its stages with large shell elements, i.e., necking, fracture initiation and propagation. As a result of softening the load will be redistributed in a smoother manner, thus removing the discontinuity of the process; terminology used in this thesis to distinguish between the sudden and softening model is presented in Figure 1.5 (B). Term damage initiation is used in the context of softening model whereas fracture initiation is used in the context of sudden model. The approach is promising and has been employed by several authors (Hogström and Ringsberg, 2012; Woelke and Abboud, 2012; Woelke et al., 2013; AbuBakar and Dow, 2013), and in a slightly modified form by Marinatos and Samuelides (2013) who replaced the softening portion of the curve with a tangent type of curve or a power law curve[5]. However, the identification of proper damage parameters which describe the softening process is a challenging task. For instance, all the authors rely on a uniaxial tensile test and assume that bifurcation from the standard true stress-strain curve occurs once the necking begins. This bifurcation point is denoted as “damage initiation” in Figure 1.5 (A). However, none of the authors describe how to account for the energy under the softening curve beyond damage initiation. Therefore, the relevant parameters that define the softening law in Figure 1.5 (A) remain unclear.

[5]Hogström and Ringsberg (2012), and AbuBakar and Dow (2013) both used an ABAQUS relative displacement approach to model damage-induced softening. Woelke and Abboud (2012), and Marinatos and Samuelides (2013) both wrote their own constitutive model.

1.3 Scope of work

This thesis enhances the fracture modeling of large-scale metal sheets with finite element method. The behavior of shell elements is considered in association with the fracture criterion that triggers their removal from the simulation. The emphasis is placed on the following aspects:

- mesh size dependence of the fracture initiation strain under multi-axial stress states;
- softening of the stress-strain curve due to necking, initiation and propagation of fracture;
- practical engineering point-of-view towards simulation of damage in ship structures.

Thus, a holistic view is taken of the fracture process, in which the fracture initiation strain depends on both the element size and the stress state in the material. Furthermore, to account for the other two stages of the material damage process, preceding necking of the material and following fracture propagation, a softening type of material relation is used. The outline of the investigation is presented in Figure 1.6.

In PI, material behavior before fracture initiation is investigated at a local scale considering pure membrane action and neglecting bending. This investigation is carried out for stress states of uniaxial (UAT), plane strain (PST), and equi-biaxial tension (EBT). Different stress states were considered since the intensity of the stress and strain gradients, and thus the severity of the mesh size effect, might depend on the stress state in the material. The phenomena that are observed are transferred onto a large scale using the concept of an averaging unit (AU). In other words, a method is proposed to determine the fracture initiation strain for sudden fracture model for large shell elements subject to various stress states. In PII softening model is introduced, fracture propagation in AU is analyzed and damage parameters for large shell elements are identified for the Mode I tearing case. In addition, softening model is implemented into the commercial code ABAQUS as a user-defined material subroutine. In PIII ductile fracture in stiffened and unstiffened panels in an idealized ship collision event is simulated using the sudden and softening model and a comparison with the existing fracture criteria is presented. In PIV the developed approach is applied to an optimized ship side structure for selected collision scenario and a comparison is made with some of the existing fracture criteria and between various mesh sizes. This illustrates the influence of the present approach on the crashworthiness predictions. PV investigates the relevant failure modes and collapse mechanisms of novel crashworthy structures, such as steel sandwich panels (Allen, 1969; Rubino et al., 2008). In

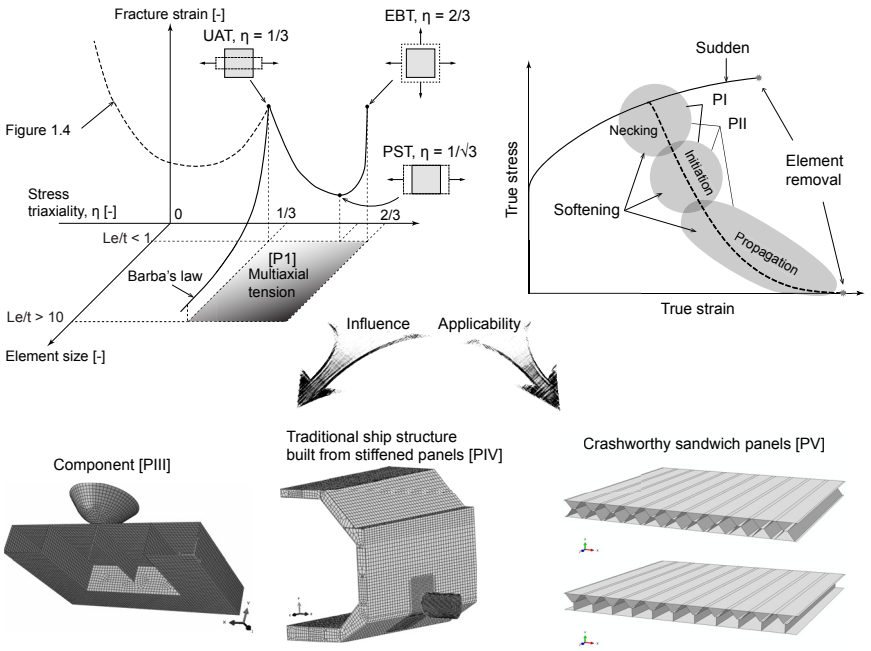

Figure 1.6. Outline of the investigation

these structures, energy is mostly absorbed by bending due to buckling and folding mechanisms, instead of fracture and tearing. This perspective brings out the limitations of the present fracture modeling approach, and thus, sets directions for future work.

1.4 Limitations

Numerical fracture simulations are challenging because of the vast number of parameters affecting the analysis (Jones, 1983; Jones, 2013), uncertainties in the input parameters (Hogström and Ringsberg, 2012; Wisniewski and Kołakowski, 2003), and the paucity of the experimental data. It is the analyst's task to identify important features of the physical phenomenon and simplify the problem accordingly. The limitations and simplifications adopted in this thesis are described below.

Ship collision and grounding accidents typically occur at low speeds so they can be considered quasi-static in nature. Therefore, all deformation processes are treated as quasi-static and the material strain-rate effects can be neglected in the analysis.

The presented approach is applicable to fracture initiation and tearing in shell elements under membrane action and out-of-plane bending is neglected. Thus, through thickness strain gradients associated with shell element bending deformations are omitted as they are considered negligible in comparison with

membrane strains in large-deformation theory where deflections are larger than $0.5t$ (Timoshenko and Woinowsky-Krieger, 1959). This limitation is justified as far as fracture in large crash simulations occur primarily under membrane loading.

Only the behavior of the basic plate and stiffener material, not that of the welded material, is considered. This is justified since the base plate tearing is a relevant failure mode during a collision or grounding event (Wang et al., 2000). Furthermore, only the behavior of steel material in room temperature is considered in this thesis.

2. Fracture modeling

2.1 Scaling of fracture initiation strain for multi-axial tension

In PI a numerical method was established to determine the fracture initiation strain and the "equivalent plane stress" material curve for large shell elements under multi-axial stress states. First, necking and fracture initiation were simulated with the fine solid element model under three different stress states: uniaxial tension (UAT), plane strain tension (PST), and equi-biaxial tension (EBT). Different stress states were considered since the intensity of the stress and strain gradients, and thus the severity of the mesh size effect, depends on the stress state in the material. The fine mesh solid element simulations employed the true stress-strain relation determined with experiments, the fracture initiation strain dependent on stress triaxiality, and the von Mises flow rule. These simulations provided the local response of the material in the localization zone that enabled the analysis of the stress state in the material, besides the strain state. To determine the size effect, fracture initiation strain, and equivalent plane stress material curve for large shell elements volume averaging was used. Hence, the local material response determined with several small solid elements ($L_e/t < 0.2$) was averaged over a predefined volume. The size (L_e/t ratio) of this averaging volume was equivalent to that of large shell elements. Through-thickness volume averaging was justified, as the thickness directional strain gradient was small in solid element simulations. This averaging volume is denoted as averaging unit (AU). Two different AU sizes were considered in order to study the effect of the mesh size on the fracture initiation strain and material curve. A distinctive feature of this upscaling method is its ability to predict the mesh dependency of the fracture initiation strain at different stress states – an important advantage over the state-of-the-art methods (Zhang et al., 1999; Simonsen and Lauridsen, 2000; Hogström et al., 2009; Ehlers and Varsta, 2009).

PI showed that the fracture initiation strain depends on the size of the averaging unit, or, effectively, on the mesh size, as well as on the stress state. In uniaxial tension the mesh size dependence is much stronger than that observed in the plane strain and equi-biaxial tension; see Figure 2.1. This proves that a Barba's law type of fracture initiation strain scaling is only valid for uniaxial

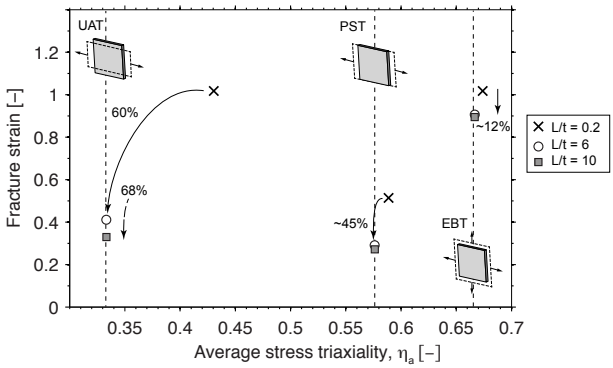

Figure 2.1. Results of PI. Mesh size effect in uniaxial tension (UAT) is much stronger than in plane strain tension (PST) and equi-biaxial tension (EBT).

tension. Therefore, the fracture initiation strain must be scaled on the basis of element size, as well as on the stress state.

Such a scaling framework was proposed by Walters (2014), who combined the closed-form necking criterion by Swift (1952) and fracture criterion applicable to small plane stress shell elements (Bai and Wierzbicki, 2010). The approach in PI delivered a generic numerical approach to obtain mesh size dependent fracture initiation strain for different stress states and justified Walters (2014) scaling framework. Thus, this scaling approach was employed in PIII. This required a calibration of stress state dependent fracture criterion applicable to small plane stress shell elements. In PIII this calibration based on the uniaxial tension test was presented, see Figure 2.2 and PIII for details.

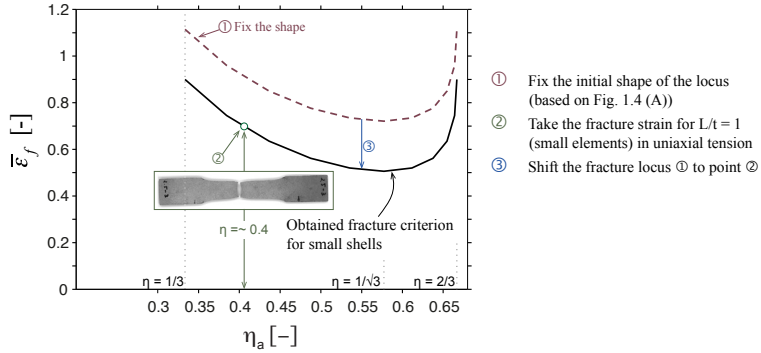

Figure 2.2. Calibration of fracture criterion for small shell elements based on uniaxial tension test.

Walters (2014) approach gives fracture initiation strain as a function of element size and stress triaxiality, i.e. $\overline{\varepsilon}_f(L_e/t, \eta)$, Figure 2.3 (A). Note how the shape of the fracture locus in Figure 2.3 (A) straightens when moving from the small scale ($L_e/t = 1$) to the large scale ($L_e/t = 8$). Consequently, the *shear* criterion, which gives the correct fracture initiation strain at a small scale only at two discrete points, provides a good estimate for the fracture initiation strain

at a macro scale in the range between uniaxial and plane strain tension. In other words, a stress state that strongly affects the fracture initiation strain in smaller elements has an almost negligible effect on the fracture initiation strain in large shell elements. With regard to large-scale collision simulations, this is an important result, which gives confidence in one of the most often used *shear* criterion for predicting fracture initiation. Using the scaling approach presented in Figure 2.3 (A) and by keeping the stress triaxiality constant, fracture strain can be plotted as a function of element size for different stress states. Figure 2.3 (B) shows similarly to Figure 2.1 how mesh size effect depends on the stress state.

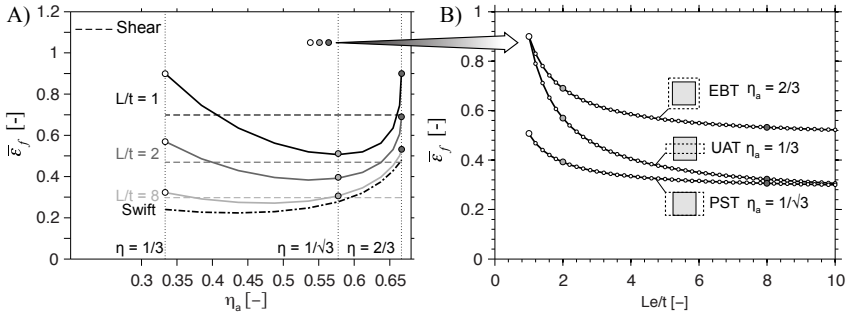

Figure 2.3. A) Scaling employed in PIII compared with shear criterion scaled with Barba's law. B) Mesh size dependence at stress states corresponding to multi-axial tension (Figure from PIII).

2.2 Damage-induced softening

PI also concluded that that the macroscopic true stress and strain relation in the case of uni-axial tension softens considerably prior to fracture initiation. The softening phenomenon was associated with the unloading of the specimen beyond through the thickness necking. In the plane strain state the softening was much weaker and in equi-biaxial tension no softening was found. It was concluded that the material relations obtained and the softening phenomenon observed are only valid until fracture initiation. Therefore, in PII the damage process and softening were investigated further and the softening model for large shell elements was devised.

2.2.1 Damage parameters

The damage parameters that define the shape of the softening material behavior were identified using the concept of a representative volume element (RVE)[6] in PII. The large-scale Mode I type of tearing experiment (crack propagates as a

[6] In the context of this thesis the concept of the RVE is equivalent to the concept of the averaging unit (AU) introduced in PI.

result of in-plane bending) previously carried out by Simonsen and Törnqvist (2004) was simulated using fine solid elements; see Figure 2.4 (A). The RVE was mapped to the crack path in the fine solid model in such a way that the crack propagated through the RVE. During the crack propagation the strain energy density in the RVE was recorded. In parallel, simulations were carried out using large shell elements, and the size of the elements was equal to the size of the RVE: $L_e/t = 2$, 6, and 10. The damage parameters were identified using an iterative approach. The assumption was that the fine solid element model correctly predicts the strain energy density for propagating cracks. This strain energy density was averaged over the RVE. The damage parameters of the softening model were iterated manually until the strain energy density distribution in large shell element corresponded to the one averaged over the RVE. The principle used for comparing the solid and shell results in the RVE is illustrated in Figure 2.4 (B).

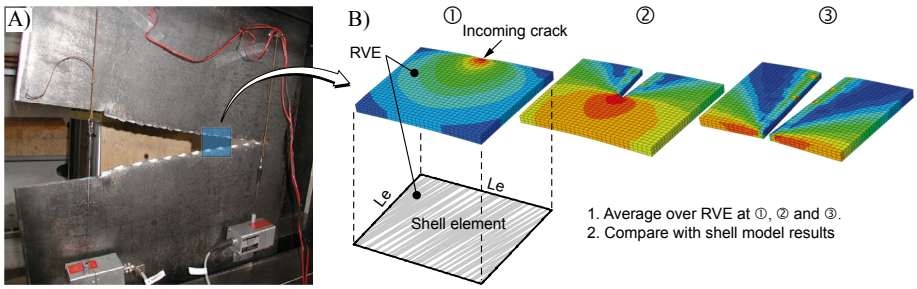

Figure 2.4. A) Mode I tearing of a large plate. Figure from (Simonsen and Törnqvist, 2004) B) Principle used for comparing the solid and shell results in the RVE at different steps.

2.2.2 Softening model

A two-stage softening model was proposed in PII to explicitly account for the necking, crack initiation, and propagation; see Figure 2.5 (A). A two-stage model permits a full control over the shape of the softening curve and was therefore suitable for a parametric study. However, the parametric study showed that the damage process of large shell elements from necking until complete failure – steps ① until ③ in Figure 2.4 (B) – can be successfully captured using only one softening stage, as shown in Figure 2.5 (B). That is, there is no need to split the softening process into two separate stages in such large-scale analysis. In the reduced model softening is induced by the damage D – a normalized quantity, which cannot be measured directly.

Damage is defined as

$$D = \int_0^{\bar{\varepsilon}_f} \frac{d\bar{\varepsilon}}{\bar{\varepsilon}_f(\eta_a)} \tag{2.1}$$

where, $\bar{\varepsilon}_f(\eta_a)$ is the fracture locus in the space of equivalent plastic strain and average stress triaxiality, for instance, as shown in Figure 2.3 (B). Therefore,

damage is a normalized indicator, which reaches the value of one, $D = 1$, when fracture initiates according to the fracture criterion. However, to account for the fact that material deterioration begins at the necking stage, the damage initiation parameter is set to be lower than one, $D_0 < 1$. To account for the fracture propagation energy element is removed after fracture initiation according to critical damage parameter, $D_c > 1$. The shape of the softening curve is controlled by the parameter m, which controls the non-linearity of the process; for details, see PII.

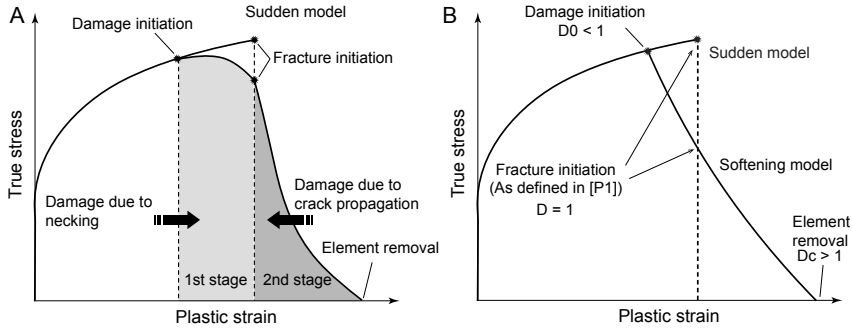

Figure 2.5. A) Two-stage softening model. B) Reduced softening model suitable for Mode I tearing in PII.

2.2.3 Influence of softening on tearing

As demonstrated in Figure 2.5 (B), the element stiffness reduces gradually with softening, which in turn resulted in a smoother force-displacement curve for the Mode I tearing problem. Although the smoother response provided by the softening model is physically more realistic, the plastic energy dissipated to tear the panel was equally well captured by the *shear* criterion and sudden model. The *shear* criterion yields a good estimate for the plastic dissipation energy for two reasons. First, it was previously calibrated by Simonsen and Törnqvist (2004) to fit the experimental results, and second, the stress state during tearing remains mostly constant.

The parametric study carried out in PII demonstrated that the amount of softening depends on the mesh size; see Figure 2.6. This effect is clearly illustrated by the area ratio: the area under the non-softened portion of the curve to the area under the softened portion. This ratio increases with decreasing element size indicating that softening loses its relevance in smaller elements. Indeed, as shown by Li and Wierzbicki (2010) and Gruben et al. (2012) softening in very small elements is only required to predict slant fracture. In the same context, the damage parameters that define the softened curve (damage initiation, critical damage, and shape) depend on the mesh size. For instance, to correctly capture the plastic dissipation energy of the structure it is critical to define the accurate value for the damage initiation parameter D_0, as well as the critical

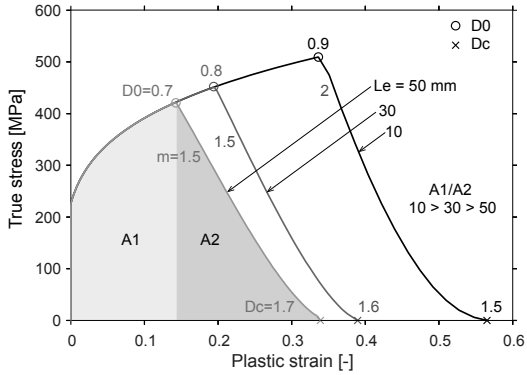

Figure 2.6. Softening models suitable for tearing simulations. Notice that the damage initiation parameter D_0 and critical damage parameter D_c are element size dependent. The shape parameter m remains constant for larger elements.

damage parameter D_c. In contrast, when damage parameters calibrated on the basis of tensile tests were employed in tearing simulations (Hogström et al., 2009; AbuBakar and Dow, 2013), the plastic dissipation energy of the structures was over- or underestimated, depending on the mesh size. With respect to structural analysis, this is a very important result. It is further pointed out that although the mesh size effect on the softening law is obvious, the results cannot explain the influence of the stress state since it remained constant throughout the tearing process. The softening model presented is valid for Mode I tearing and therefore, the applicability of the present approach to actual structures is discussed in detail in the next chapter.

3. Influence on structural response

3.1 Stiffened and unstiffened panels

3.1.1 Experiments and FE analysis

To determine the influence of the findings from papers PI and PII on the finite element crashworthiness analysis, panel indentation simulations were carried out in PIII. The influences of mesh size, stress states and softening on impact simulations were studied. FE simulations were carried out with the stiffened and unstiffened panels. Panels were experimentally tested (Alsos and Amdahl, 2009) and later analyzed by Alsos et al. (2009) using BWH and RTCL damage criteria. The experimental setup is shown in Figure 3.1. The FE models were discretized with a wide range of element sizes ranging from $L_e/t = 1...20$. The fracture initiation strain was scaled on the basis of the stress state and element size according to Figure 2.3 (A)[7]. Softening was used in the context of the largest shell elements $L_e/t = 20$ and the results were compared with the sudden model. The fracture criterion and softening were only defined for the plate since fracture did not occur in the stiffener in the experiments. Simulations were also carried out with the *shear* fracture criterion adjusted for different element sizes according to Barba's law.

3.1.2 Influence of mesh size on panel response and fracture prediction

Compared with the analysis carried out with the *shear* criterion and the results obtained by Alsos et al. (2009) with the RTCL criterion, the present scaling approach delivered more accurate results regarding the measured and simulated force-displacement curves for a wide range of element sizes. The mesh size dependency of the FE solution was reduced in comparison with other approaches since the stress state is considered in scaling the fracture initiation strain. The *shear* and RTCL criteria could provide good agreement between the measured

[7] In the experiments the plate thickness in the panels was 5 mm; thus this thickness was also used in the simulations. Although Figure 2.3 gives the fracture initiation strain as a function of the dimensionless element size L_e/t, the results presented in the following section will apply only to the plate thickness of 5 mm.

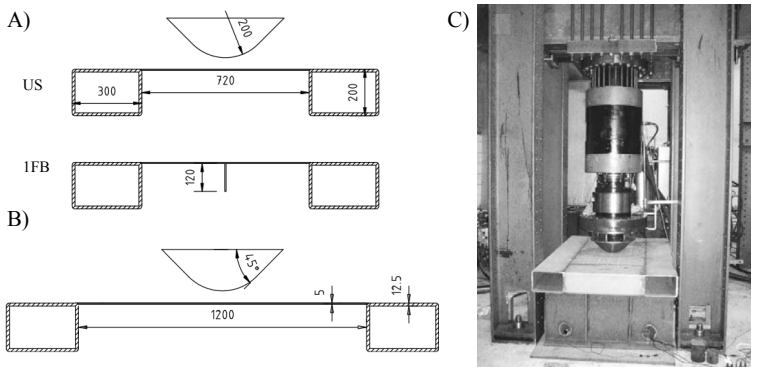

Figure 3.1. A) Transverse and B) longitudinal cross-sections of the panels with and without stiffener. c) Experimental setup illustrating the equipment (rig, hydraulic jack and test component). Figures from Alsos and Amdahl (2009).

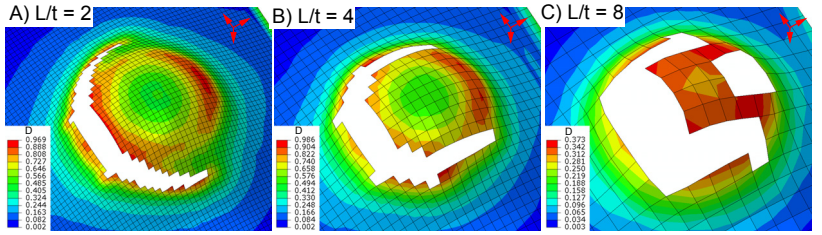

Figure 3.2. Contours of damage at the fracture location obtained with different mesh densities – US panel, [PIII]. A) $L_e/t = 2$. B) $L_e/t = 4$. C) $L_e/t = 8$.

and simulated force-displacement curves for a specific element size. However, this accuracy was not preserved when the element size was changed. It is worth noting that Alsos et al. (2009) also obtained mesh-independent results when employing the BWH criterion, but an unstiffened panel, for instance, failed earlier when this criterion was used.

Figure 3.2 presents the damage contours of the failed panels obtained with the present approach. In the test, the crack propagated in a direction that required the lowest amount of energy, which had a trajectory of the circumference. In spite of the rectangular mesh employed, current simulations can approximate the annular crack path. The behavior is most accurately reproduced by the smallest elements $L_e/t = 2$ in Figure 3.2 (A), where the annular crack clearly prevails. In simulations with larger elements $L_e/t = 4$ and 8 the size of the elements and orthogonality of the mesh forces the crack to grow along a straight path in the longitudinal direction of the panel. Eventually, the crack will turn because of the mechanics of the problem, but still prefers to propagate along a straight path. In the current case, crack propagating along a straight path will increase the energy absorbed by the structure.

3.1.3 Influence of softening on panel response and fracture prediction

The panels carried loads primarily through membrane action, which led to a sudden loss of stiffness once the failure happened. The resulting load drop was steep and since the softening mostly affects the analysis beyond fracture initiation and during fracture propagation, it had a minor influence on the current analyses. Although the crack propagated in the experiments, the element size in these simulations was so large that the whole force-displacement response was completely defined by the removal of a single large element; see Figure 3.3 (B) and (C). Nevertheless, one difference between the sudden and softening models was that the elements were kept longer in the simulation with softening; see, for example, the unstiffened panel results in Figure 3.3. Considering the series of events taking place during the ship collision or grounding analysis, keeping elements in the analysis longer can affect the extent of the damage, the amount of water flowing in, and consequently the survivability of the ship (Spanos and Papanikolaou, 2011; Ringsberg, 2010).

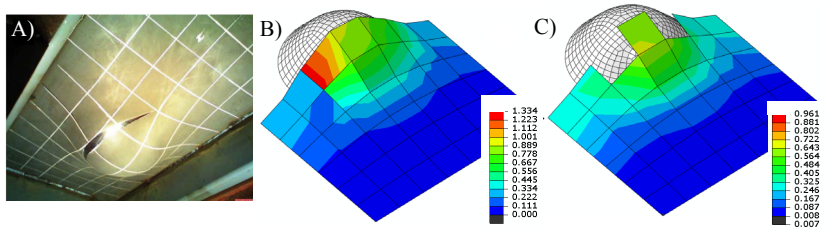

Figure 3.3. Unstiffened panel. A) Experiment (Alsos and Amdahl, 2009). B) Analysis results with softening model and C) sudden model. Damage contours are shown, [PIII].

Furthermore, the damage parameters calibrated in PII for the stable tearing process were modified to capture the experimental force-displacement curve and sudden force drop in panels after fracture initiation. In effect, the softening part of the material relation changed as shown in Figure 3.4. Note that in the case of Mode I tearing the stress reduction was almost linear ($m = 1.5$), whereas in the panel simulations it is logarithmic ($m = 3$). In contrast, other authors have mainly used linear, $m = 1$ (AbuBakar and Dow, 2013; Hogström and Ringsberg, 2012), or exponential stress reduction, $m < 1$ (Woelke and Abboud, 2012). Figure 3.4 reveals that in the panel indentation simulations (PIII) less softening was required than in the tearing simulations (PII). This is an important result given that the main aim of the softening is to correctly capture the plastic dissipation energy of large shell elements during the damage process, whereas this damage process as shown depends on the failure mode in tearing. Here, two contrasting failure modes are noted: a stable tearing process observed in PII versus the fracture initiation and sudden rupture of the plating accompanied by the significant load drop observed in PIII. Besides the

different failure modes, the stress state also varied between the two simulations: in the panel simulations the stress state was between the plane strain and equi-biaxial tension, while in the tearing simulations (PII) it was between the plane strain and uniaxial tension. This implies that the amount of softening is related to the stress state in the material. This is also supported by the results of PI, which showed that the damage-induced softening prior to initiation was at its strongest in uniaxial tension.

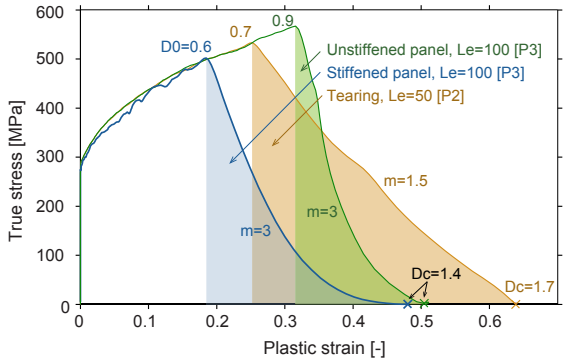

Figure 3.4. Amount of softening represented by the area under the softening portion of the curve in different analysis.

3.1.4 Discussion on importance

Based on the FE tearing simulations carried out in PII and impact simulations carried out in PIII the importance of softening is discussed in the context of stiffened panel analysis. It is certainly attractive to phenomenologically model necking, fracture initiation and propagation inside large shell elements with softening. However, in some cases the difficulties related to calibration of damage parameters outweigh the benefits. Analyses show that the damage parameters depend on the stress state, failure mode (stable tearing vs. sudden fracture initiation) and mesh size, which makes the analysis overly complicated for practicing engineer. In contrast, traditional sudden model is shown to give reasonable results with different mesh densities (PIII) as far as the fracture initiation strain is properly scaled on the basis of mesh size and stress state, Figure 2.3 (A).

3.2 Large-scale structures

3.2.1 Collision simulations with different criteria

Softening had a minor influence on the analysis results in the panel indentation simulations. This was due to limited damage size and the fact that only one

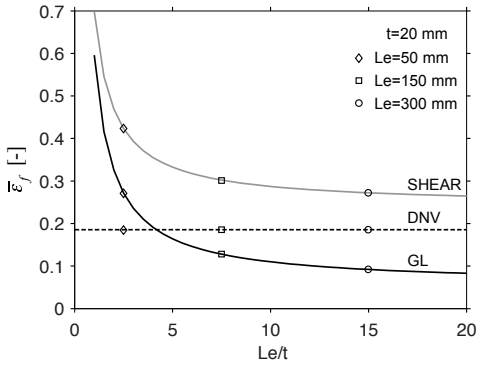

Figure 3.5. Fracture criteria employed.

large shell element was removed in the analysis. For this reason, the extent of the damage had to be increased to demonstrate the effect of softening on large-scale crash simulations. Therefore, in PIV collision simulations were carried out with a ship side structure that had previously been optimized for crashworthiness by Kõrgesaar and Ehlers (2010). In those simulations element length was 150 mm and approximately 500 shell elements were removed. The structure was analyzed with 3 different state-of-the-art fracture criteria (sudden models): the *shear* criterion, the DNV (2013) constant fracture initiation strain criterion, which is independent of the element size and stress state, and the critical through thickness strain criterion referred to as GL (Zhang et al., 2004; Scharrer et al., 2002); see Figure 3.5. Additionally, the present approach was used, in which the fracture initiation strain depends on both the mesh size and stress state according to Figure 2.3. With regard to the present approach, both the sudden model and the softening model were employed. In simulations with softening model the same set of damage parameters was used as defined in PIII for the stiffened panel.

To determine how the criteria employed can handle the mesh size effect different mesh sizes were considered. The effect of the mesh size on the crash and collapse analysis of large structures has been discussed by various authors, e.g., Amdahl and Kavlie (1992), Naar (2006), Paik (2007a), and Paik (2007b). The mesh size should be fine enough to capture the primary damage mechanisms observed in ship collision analysis: membrane stretching, bending due to folding, and crushing of the main supporting members (Wang et al., 2000). Naar (2006) reports that to simulate collapse, at least four shell elements have to be used for plating between stiffeners, whereas Kitamura (2000) states that a 200-mm element size is a standard for a side shell collision. Therefore, the structures were discretized with three different element lengths at the collision location: 50, 150, and 300 mm[8], which resulted in ~14, ~5, and 2 elements between

[8]Here the elements are quoted by their length instead of their dimensionless size L_e/t as the plate thickness at the impact location varied from 20 mm to 28 mm.

the stiffeners, respectively. It is pointed out that 300-mm mesh was selected deliberately larger than suggested in the literature so as to test the limits of the present approach.

3.2.2 Comparison of different criteria

The plastic dissipation energy obtained with different criteria and mesh sizes is presented in Figure 3.6. It was found that most of the elements fail in stress states between uniaxial ($\eta = 1/3$) and plane strain tension ($\eta = 1/\sqrt{3}$). As shown in Figure 3.6 (A), the present approach with softening converges to the same solution independent of whether 50 or 150 mm elements were used. This shows that softening is necessary to account for the mesh size effect in this particular case. In contrast, the mesh size effect is clearly present in the 300-mm element solution, demonstrating once more that the amount of softening is mesh size dependent. This coarse mesh cannot capture the plate collapse mechanism between the stiffeners nor the folding and tripping of the stiffeners. Such deficiencies and structural strengthening cannot be accounted for even with the softening material curve devised to characterize the damage process of large shells from necking until complete failure, excluding other mechanisms such as bending. As a result, force-displacement curves obtained with 300 mm mesh displayed strong oscillations and were not informative.

The present approach without softening (Figure 3.6 (B)) does not show the same convergence as obtained with softening: 150 mm solution is shown to absorb more energy than 50 mm solution. It is pointed out that number of elements that failed was the same in the analysis with and without softening. This suggests that in analysis without softening, fracture strain should have been even lower. Similar conclusion is appropriate also for the *shear* criterion, which overestimates the absorbed energy with 150 mm mesh in comparison with 50 mm mesh, see Figure 3.6 (C).

The DNV criterion, on the other hand, yielded a low scatter band between the different mesh sizes, as evidenced in Figure 3.6 (D). However, this is attributed to the low fracture initiation strain value, as a result of which elements were removed before the mesh size effect settled in[9]. For the same reason, the dissipated plastic energy is the most conservative in comparison with the other criteria, although the number of elements removed, for instance in the 150-mm model, was twice as high as that predicted with the present approach. This suggests that the extent of the damage is also considerably larger. At the same time, the plastic dissipation energy obtained with the coarsest, 300 mm mesh, was closest to the reference solution (the present approach with softening, $L_e = 50$ mm).

Figure 3.6 (E) shows that the GL criterion considers the mesh dependency

[9] It is reminded here that the FE solution becomes mesh size dependent beyond necking.

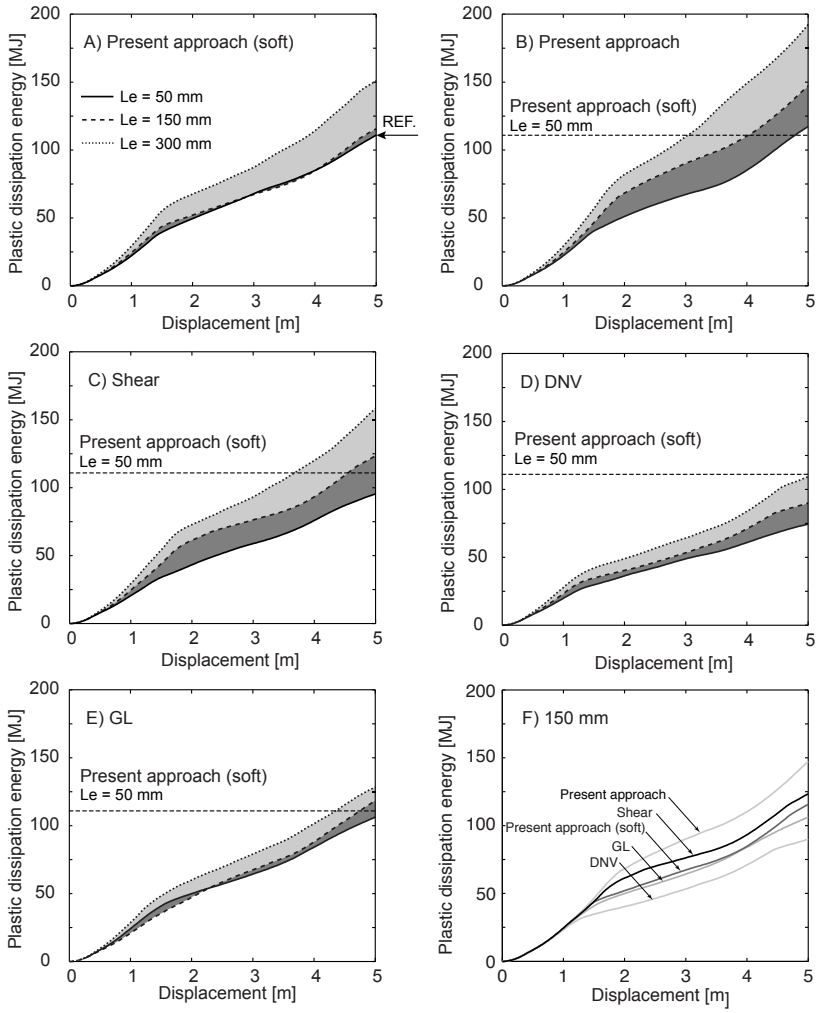

Figure 3.6. Scatter band in plastic dissipation energy obtained with different fracture criteria.

effectively in both coarse mesh models, whereas the convergence compared with the reference solution is very good. However, it was expected that less energy will be absorbed in comparison with the DNV criterion as the GL fracture strain is lower than that given by the DNV criterion, Figure 3.5. The low fracture initiation strain explains why the mesh size effect did not appear in simulations with GL and DNV criteria. However, to explain why more energy was dissipated in the analysis compared with the DNV criterion a closer look was taken at the failed elements. It was found that, compared with other criteria, fewer elements failed in stress states below a stress triaxiality $\eta = 1/3$ characterizing uniaxial tension. The reason is that thinning of the material is not a dominant mechanism in $\eta < 1/3$, i.e., in shear and compression. Hence, the critical thinning strain criterion cannot predict failure in this region. As a result, since elements are not removed, the energy dissipated on deforming

them is significantly higher than in other cases. By coincidence, the plastic dissipation energy is similar to that obtained with the present approach with softening and the 50-mm model.

Figure 3.6 (F) compares the results obtained with different criteria and 150 mm mesh. The present scaling approach (sudden model) provides an upper bound and DNV criterion a lower bound for the scatter band. The rest of the criteria provide a comparable estimate for the plastic dissipation energy and in terms of accuracy no preference between different criteria can be made.

3.2.3 Failure mechanisms in novel energy absorbing structures

Commonly, ship structures are built from stiffened panels. Large deflections in stiffened panels lead to situation where the membrane state dominates over the bending. This makes the present approach developed for multi-axial tension suitable for stiffened panels, as shown in PIII and PIV where the mesh size dependency is removed to a better extent than with the state-of-the-art methods.

However, in recent years novel crashworthy structures, such as various sandwich panels, have been proposed where the majority of the impact energy is absorbed through in-plane stretching, plastic hinge formation and folding to avoid early-stage rupture (Naar et al., 2002; Klanac et al., 2005; Pedersen et al., 2006; Karlsson, 2009). These bending-governed structures are more efficient in spreading the impact load over a wider area. In PV it was shown that optimal core geometry could further increase the energy-absorbing capabilities of these structures without the weight penalty. The main finding was that it is desirable to initiate early-stage buckling and plastic hinge formation in the core to allow load redistribution into adjacent structural members. This leads to a softer response compared with stiffened panels. Therefore, the key difference compared with stiffened panels is that most of the impact energy is absorbed through crushing (folding and buckling) of the core as shown in Figure 3.7 (A), as opposed to fracture and tearing. To capture these mechanisms in the core a relatively fine mesh is needed, as large shells cannot model such complicated

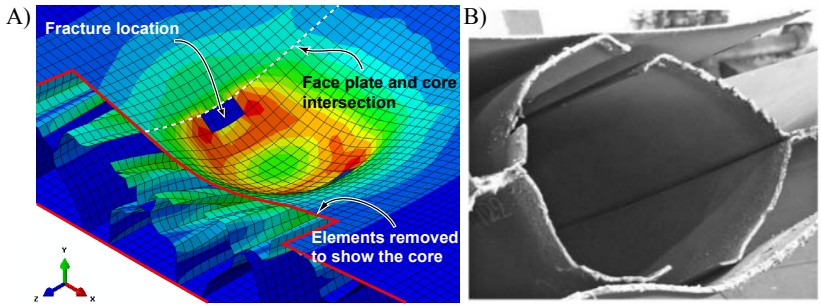

Figure 3.7. A) Deformation mechanism in optimized X-core sandwich panel. B) Picture of the failed laser weld in the X-core sandwich panel. Figure from Ehlers et al. (2012).

deformation modes. Moreover, the fracture takes place in the vicinity of the intersection between the face plates and core, Figure 3.7 (A). In real structures welds are located at these intersections. Such failure mode along longitudinal welds was also reported by Ehlers et al. (2012), see Figure 3.7 (B). The present approach however, is validated for the base plate material. Furthermore, such joint-failure includes local out-of-plane bending and thus, through thickness strain gradients. Because of these reasons the applications of the approaches that neglect strain gradients due to bending to structures where the bending occurs in the vicinity of welds is questionable; such structures are for example the steel sandwich panels [PV].

4. Concluding remarks

There were two main aims in this thesis. First, to understand the damage process of large shell elements considering the phenomena observed in small-scale test specimens such as necking, consequential softening and ultimate ductile fracture. Second, to explore a rational and practical way to simulate the damage of ship structures using large shell elements. Until now, the influence of such local phenomena on the behavior of large shell elements has not been explicitly analyzed. The damage process of shell elements was divided into three stages: necking, fracture initiation, and fracture propagation. A softening type of true stress and strain curve was used in order to describe the macroscopic response of large shell elements. The approach presented was compared against other state-of-the-art methods in sample simulations of panel indentation tests and ship collisions.

In PI a numerical method was developed that defines the equivalent plane stress material curve until fracture initiation strain for large shell elements under multi-axial tension. It was found that the fracture initiation strain scales according to the stress state. The results show that the stress state has only minor influence on the fracture initiation strain of large shell elements, especially between the uniaxial and plane strain tension. The importance of this finding is emphasized due to the fact that elements failed mostly between those two stress states in ship collision simulation [PIV]. In the context of large-scale crash simulations, the above result gives confidence in criteria that neglect the stress state, e.g., the *shear* criterion. On the other hand, stress state has a major influence on the fracture strain scaling. Significance of this discovery is expected to increase over the coming years with ever increasing computational power that paves the way for exploiting finer meshes even in very large structures, such as ships.

Softening type of stress-strain curve was introduced in PII to phenomenologically describe necking, fracture initiation and propagation with large shell elements under tension. Analyses with the softening model in PII showed that, in contrast to the sudden model, strain energy density distribution in the failing shell elements can be captured accurately. As indicated in PIV softening also helps to get better convergence with larger shell elements, i.e. remove mesh size effect. However, it is very complicated to define proper calibration parameters a priori for real structures. Even for a simple tearing case under in-plane bending, calibration of parameters required several iterations (PII). These parameters

depend on the mesh size, the load experienced by the element and how this changes as the failure progresses within the element, as demonstrated in PII and PIII. This means that commonly applied calibration approach on the basis of a tensile test, see e.g. (Hogström et al., 2009; Woelke and Abboud, 2012; Woelke et al., 2013; AbuBakar and Dow, 2013), is insufficient.

However, from practical engineering point-of-view the importance in crashworthiness analysis is on absorbed energy of the structure. Thus, existing sudden models (calibrated for absorbed energy) give reasonable results and are easier to use than the softening type of model. In these cases the softening model can be impractical considering the gained accuracy and convergence. When considering also bending induced through-thickness strain gradient, through which energy is absorbed in novel crashworthy structures (PV), the calibration would become even more complex. This means that the sudden models become even more attractive for practical engineering work.

In a future work, the present scaling approach should be extended and validated for other stress states besides multi-axial tension, different materials (e.g. aluminum, welds, high strength steels) and temperatures. To account for bending induced thickness directional strain gradients, a layer-wise averaging approach should be developed. In addition, experimental research utilizing Digital Image Correlation should be carried out to measure the strain gradients and to investigate in detail the failure process of material under multi-axial loading. Averaging experimental results would definitely add confidence of using shell elements in ship collision and grounding simulations. There are situations where the strain rate becomes an important factor (explosions etc). In principle, the present methodology could be extended in that direction. Arctic environment sets challenges for material modeling. Thus, experimental and computational investigations should be carried out to extend the methodology in this direction. However, all these aspects are also left for future work.

Errata

Publication II

On p. 4 instead of Table 1 read Table 2

Publication III

On p. 14, Chapter 5, second paragraph: instead of Figs. 10(a) and 14(a) read Figs. 11(a) and 15(a). In Figure 17 a) the damage legends should be vice-versa as shown in manuscript Figure 3.3.

Publication IV

Two errors in captions to figures. Figure 9 should read Figure 10, and Figure 10 should read Figure 11. Because of that, there are two errors in references to the figures. On p.6, last paragraph: instead of Fig. 10 read Fig. 11. On p.7, last paragraph of Chapter 6: instead of Fig. 8 (c) read Fig. 9(c).

Bibliography

ABAQUS, 2011. ABAQUS Analysis User's Manual, Version 6.11, Dassault Systemes Simulia Corporation.

AbuBakar, A. and Dow, R.S., 2013. Simulation of ship grounding damage using the finite element method. Int. J. Solids Struct., 50(5), pp. 623–636.

Allen, H.G., 1969. In: Analysis and Design of Structural Sandwich Panels Pergamon Press, Oxford.

Alsos, H.S. and Amdahl, J., 2009. On the resistance to penetration of stiffened plates, Part I – Experiments. Int. J. Impact Eng., 36(6), pp. 799–807.

Alsos, H.S., Amdahl, J. and Hopperstad, O.S., 2009. On the resistance to penetration of stiffened plates, Part II: Numerical analysis. Int. J. Impact Eng., 36(7), pp. 875–887.

Alsos, H.S., Hopperstad, O.S., Törnqvist, R. and Amdahl, J., 2008. Analytical and numerical analysis of sheet metal instability using a stress based criterion. Int. J. Solids Struct., 45(7-8), pp. 2042–2055.

Amdahl, J. and Kavlie, D., 1992. Experimental and numerical simulation of double hull stranding, DNV – MIT Workshop.

Bai, Y. and Wierzbicki, T., 2010. Application of extended Mohr–Coulomb criterion to ductile fracture. Int. J. Fract., 161(1), pp. 1–20.

Bai, Y., 2008. Effect of Loading History in Necking and Fracture. Thesis (Ph. D.). Massachusetts Institute of Technology, Dept. of Mechanical Engineering.

Bao, Y. and Wierzbicki, T., 2004. A Comparative Study on Various Ductile Crack Formation Criteria. J. Eng. Mater. Technol., 126(3), pp. 314-324.

Barenblatt, G.I., 1962. The mathematical theory of equilibrium cracks formed in brittle fracture. Advances in Applied Mechanics. 7, pp. 55-129

Barsoum, I. and Faleskog, J., 2007. Rupture mechanisms in combined tension and shear—Experiments. Int. J. Solids Struct., 44(6), pp. 1768–1786.

Benzerga, A. and Leblond, J.-B., 2010. Ductile fracture by void growth to coalescence. Advances in applied Mechanics, 44, pp.169–305.

Choung, J., Shim, C.-S. and Song, H.-C., 2012. Estimation of failure strain of EH36 high strength marine structural steel using average stress triaxiality. Mar. Struct., 29(1), pp. 1–21.

Coenen, E.W.C., Kouznetsova, V.G. and Geers, M.G.D., 2012. Multi-scale continuous–discontinuous framework for computational-homogenization–localization. J. Mech. Phys. Solids, 60(8), pp.1486–1507.

Det Norske Veritas, DNV-RP-C208: 2013. Determination of Structural Capacity by Non-linear FE Analysis Methods, pp. 1–66.

Dugdale, D.S., 1960. Yielding of steel sheets containing slits. J. Mech. Phys. Solids, 8(2), pp.100–104.

Dunand, M. and Mohr, D., 2014. Effect of Lode parameter on plastic flow localization after proportional loading at low stress triaxialities. J. Mech. Phys. Solids, 66(C), pp.133–153.

Ehlers, S., 2010. A procedure to optimize ship side structures for crashworthiness. Proceedings of the Institution of Mechanical Engineers, Part M: Journal of Engineering for the Maritime Environment, 224(1), pp. 1–11.

Ehlers, S. and Varsta, P., 2009. Strain and stress relation for non-linear finite element simulations. Thin. Wall. Struct., 47(11), pp. 1203–1217.

Ehlers, S., Tabri, K., Romanoff, J. and Varsta, P., 2012. Numerical and experimental investigation on the collision resistance of the X-core structure. Ships and Offshore Structures, 7(1), pp.21–29.

Garrison, W.M., Jr and Moody, N.R., 1987. Ductile fracture. Journal of Physics and Chemistry of Solids, 48(11), pp.1035–1074.

Geers, M.G.D., Kouznetsova, V.G. and Brekelmans, W.A.M., 2010. Multi-scale computational homogenization: Trends and challenges. Journal of Computational and Applied Mathematics, 234(7), pp.2175–2182.

Gruben, G., Hopperstad, O.S. and Børvik, T., 2012. Simulation of ductile crack propagation in dual-phase steel. Int. J. Fract., 180(1), pp. 1–22.

Gurson, A.L., 1977. Continuum Theory of Ductile Rupture by Void Nucleation and Growth: Part I—Yield Criteria and Flow Rules for Porous Ductile Media. J. Eng. Mater. Technol., 99(1), pp.2–15.

Haltom, S.S., Kyriakides, S. and Ravi-Chandar, K., 2013. Ductile failure under combined shear and tension. Int. J. Solids Struct., 50(10), pp. 1507–1522.

Hogström, P. and Ringsberg, J.W., 2012. An extensive study of a ship's survivability after collision – A parameter study of material characteristics, non-linear FEA and damage stability analyses. Mar. Struct., 27(1), pp. 1–28.

Hogström, P., Ringsberg, J.W. and Johnson, E., 2009. An experimental and numerical study of the effects of length scale and strain state on the necking and fracture behaviours in sheet metals. Int. J. Impact Eng., 36(10-11), pp. 1194–1203.

IMO (2006) Resolution MSC.216 (82) Adoption of Amendments to the International Convention for the Safety of Life at Sea, 1974, as amended, December 8

ISSC, 2006. Report of committee V1: collision and grounding. In: P.A. Frieze, R.A. Shenoi, editors. Proceedings of the 16th International Ship and Offshore Structures Congress, Southampton, UK.

Johnson, G.R. and Cook, W.H., 1985. Fracture characteristics of three metals subjected to various strains, strain rates, temperatures and pressures. Eng. Fract. Mech., 21(1), pp. 31–48.

Jones, N., 1983. Structural aspects of ship collisions. Structural crashworthiness, Chapter 11. Butterworth & Co (Publishers) Ltd.

Jones, N., 2013. The credibility of predictions for structural designs subjected to large dynamic loadings causing inelastic behaviour. Int. J. Impact Eng., 53, pp. 106–114.

Karlsson, U.B., 2009. Improved collision safety of ships by an intrusion-tolerant inner side shell. Marine Technology, 46(3), pp. 165–173.

Kitamura, O., 2000. Buffer Bow Design for the Improved Safety of Ships. Proceedings of the SSC/SNAME/ASNE Symposium, Society of Naval Architects and Marine Engineers.

Klanac, A. et al., 2005. Qualitative design assessment of crashworthy structures. Proceedings of the International Maritime Association of Mediterranean, Portugal, pp. 461–469.

Lemaitre, J., 1985. A Continuous Damage Mechanics Model for Ductile Fracture. J. Eng. Mater. Technol., 107(1), p.83.

Lemaitre, J., 1996. A Course on Damage Mechanics, Springer.

Li, Y. and Wierzbicki, T., 2010. Prediction of plane strain fracture of AHSS sheets with post-initiation softening. Int. J. Solids Struct., 47(17), pp. 2316–2327.

Lou, Y., Huh, H., Lim, S. and Pack, K., 2012. New ductile fracture criterion for prediction of fracture forming limit diagrams of sheet metals. Int. J. Solids Struct., 49(25), pp. 3605–3615.

Marinatos, J.N. and Samuelides, M., 2013. Material characterization and implementation of the RTCL, BWH and SHEAR failure criteria to finite element codes for the simulation of impacts on ship structures. J. Amdahl, S. Ehlers, and B. J. Leira, eds. Collision and Grounding of Ships and Offshore Structures. CRC Press, Trondheim, Norway, pp. 57–67.

McClintock, F.A., 1968. A criterion for ductile fracture by the growth of holes. J. Appl. Mech., 35, pp. 363–371.

Naar, H., 2006. Ultimate Strength Of Hull Girder For Passenger Ships. Doctoral thesis. Helsinki University of Technology.

Naar, H., Kujala, P., Simonsen, B.C. and Ludolphy, H., 2002. Comparison of the crashworthiness of various bottom and side structures. Mar. Struct., 15(4), pp. 443–460.

Nielsen, K.L. and Hutchinson, J.W., 2012. Cohesive traction-separation laws for tearing of ductile metal plates. Int. J. Impact Eng., 48(C), pp.15–23.

Paik, J.K., 2007a. Practical techniques for finite element modeling to simulate structural crashworthiness in ship collisions and grounding (Part I: Theory). Ships and Offshore Structures, 2(1), pp. 69–80.

Paik, J.K., 2007b. Practical techniques for finite element modelling to simulate structural crashworthiness in ship collisions and grounding (Part II: Verification). Ships and Offshore Structures, 2(1), pp. 81–85.

Pedersen, C.B.W., Deshpande, V.S. and Fleck, N.A., 2006. Compressive response of the Y-shaped sandwich core. Eur. J. Mech. A-Solid., 25(1), pp. 125–141.

Rees, D., 2006. Basic Engineering Plasticity: An Introduction with Engineering and Manufacturing Applications 1st ed, Butterworth-Heinemann.

Rice, J.R. and Tracey, D.M., 1969. On the ductile enlargement of voids in triaxial stress fields*. J. Mech. Phys. Solids, 17(3), pp. 201–217.

Ringsberg, J.W., 2010. Characteristics of material, ship side structure response and ship survivability in ship collisions. Ships and Offshore Structures, 5(1), pp. 51–66.

Rubino, V., Deshpande, V.S. and Fleck, N.A., 2008. The collapse response of sandwich beams with a Y-frame core subjected to distributed and local loading. Int. J. Mech. Sci., 50(2), pp.233–246.

Samuelides, M., 2012. Designing for protection against collision. C. Guedes Soares, Y. Garbatov, N. Fonseca, and A. P. Texeira, eds. Marine Technology and Engineering. pp. 955–977.

Scharrer, M., Zhang, L. and Egge, E.D., 2002. Collision calculations in naval design systems, Report. Final report MTK0614 Nr. ESS2002.183, Version 1/2002-11-22, Germanischer Lloyd, Hamburg.

Scheider, I. and Brocks, W., 2006. Cohesive elements for thin-walled structures. Comp. Mater. Sci., 37(1-2), pp.101–109.

Simonsen, B.C. and Törnqvist, R., 2004. Experimental and numerical modelling of ductile crack propagation in large-scale shell structures. Mar. Struct., 17(1), pp. 1–27.

Simonsen, B.C. and Lauridsen, L.P., 2000. Energy absorption and ductile failure in metal sheets under lateral indentation by a sphere. Int. J. Impact Eng., 24(10), pp. 1017–1039.

Spanos, D.A. and Papanikolaou, A.D., 2011. On the time dependence of survivability of ROPAX ships. J Mar Sci Technol, 17(1), pp. 40–46.

Swift, H.W., 1952. Plastic instability under plane stress. J. Mech. Phys. Solids, 1(1), pp. 1–18.

Tardif, N. and Kyriakides, S., 2012. Determination of anisotropy and material hardening for aluminum sheet metal. Int. J. Solids Struct., 49(25), pp. 3496–3506.

Tasan, C.C., Hoefnagels, J.P.M., Horn, ten, C.H.L.J. and Geers, M.G.D., 2009. Experimental analysis of strain path dependent ductile damage mechanics and forming limits. Mechanics of Materials, 41(11), pp.1264–1276.

Timoshenko, S.P. and Woinowsky-Krieger, S., 1959. Theory of plates and shells, 2nd edition, McGraw-Hill, New York.

Tvergaard, V., 2015. Effect of initial void shape on ductile failure in a shear field. Mechanics of Materials, pp.1–8.

Törnqvist, R., 2003. Design of Crashworthy Ship Structures. Doctoral thesis. DTU.

Urban, J., 2003. Crushing and Fracture of Lightweight Structures. Doctoral thesis. Technical University of Denmark.

Villavicencio, R., Liu, B. and Soares, C.G., 2013. Response of a tanker side panel punched by a knife edge indenter. J. Amdahl, S. Ehlers, and B. J. Leira, eds. Collision and Grounding of Ships and Offshore Structures. Trondheim, Norway, pp. 109–115.

Walters, C.L., 2014. Framework for adjusting for both stress triaxiality and mesh size effect for failure of metals in shell structures. Int. J. Crashworthines, 19(1), pp. 1–12.

Wang, G., Arita, K. and Liu, D., 2000. Behavior of a double hull in a variety of stranding or collision scenarios. Mar. Struct., 13(3), pp.147–187.

Wattrisse, B., Chrysochoos, A., Muracciole, J.-M. and Némoz-Gaillard, M., 2001. Kinematic manifestations of localisation phenomena in steels by digital image correlation. Eur. J. Mech. A-Solid., 20(2), pp.189–211.

Wierzbicki, T., Bao, Y., Lee, Y.-W. and Bai, Y., 2005. Calibration and evaluation of seven fracture models. Int. J. Mech. Sci., 47(4-5), pp.719–743.

Wiśniewski, K. and Kołakowski, P., 2003. The effect of selected parameters on ship collision results by dynamic FE simulations. Finite Elements in Analysis and Design, 39(10), pp.985–1006.

Woelke, P.B. and Abboud, N.N., 2012. Modeling fracture in large scale shell structures. J. Mech. Phys. Solids, 60(12), pp. 2044–2063.

Woelke, P.B., Shields, M.D., Abboud, N.N. and Hutchinson, J.W., 2013. Simulations of ductile fracture in an idealized ship grounding scenario using phenomenological damage and cohesive zone models. Comp. Mater. Sci., 80, pp. 79–95.

Zhang, L., Egge, E.D. and Bruhms, H., 2004. Approval procedure concept for alternative arrangements. Proceedings of the 3rd International Conference on Collision and Grounding of Ships (ICCGS2004), Izu, Japan.

Ship collisions and groundings are one of the greatest operational risks in maritime transportation. Regardless of continuous efforts to prevent these accidents, they will remain a serious threat. In order to minimize the consequences of such serious accidents engineers have to take into account the accidental loading in the design process. As a result of accidental loading, thin-walled ship structures fail due to fracture and tearing. This thesis investigates how to model these phenomena with finite element method and shell elements.

Aalto-DD 22/2015

ISBN 978-952-60-6084-2 (printed)
ISBN 978-952-60-6085-9 (pdf)
ISSN-L 1799-4934
ISSN 1799-4934 (printed)
ISSN 1799-4942 (pdf)

Aalto University
School of Engineering
Department of Applied Mechanics
www.aalto.fi